https://doi.org/10.30799/jnst.280.20060102 J. Nanosci. Tech. - Volume 6 Issue 1 (2020) 866–868

Share Your Innovations through JACS Directory

Journal of Nanoscience and Technology

Visit Journal at http://www.jacsdirectory.com/jnst

ISSN: 2455-0191

Low Temperature Hydrogen Gas Sensing Performance of Fe-doped SnO_2 Nanostructured Thin Films

S.V. Jagtap[1], A.S. Tale[1], S.D. Thakre[1], M.J. Pawar[2,*]

[1]*Department of Physic, R.D.I.K College, Badnera Rly. – 444 701, Maharashtra, India.*
[2]*Laboratory of Materials Synthesis, Department of Chemistry, ACS College, Kiran Nagar, Amravati – 444 602, Maharashtra, India.*

ARTICLEDETAILS

Article history:
Received 29 July 2019
Accepted 27 September 2019
Available online 22 January 2020

Keywords:
Hydrogen Sensor
SnO_2 Thin Films
Gas Sensors
Sol-Gel
Fe Doped SnO_2

ABSTRACT

Fe doped tin oxide was prepared by hydrothermal method and the same has been used to fabricate a thin film for sensing. Fe doped tin oxide was prepared by sol–gel dip-coating technique on the glass substrates for hydrogen sensing. The microstructure and morphology of the prepared materials were analysed by XRD and SEM analysis. The SEM images clearly show that doping can clamp down the growth of the large crystallites and can lead to large agglomeration spheres. Thin film gas sensors were formed from undoped pure SnO_2 and Fe doped SnO_2. The sensors were exposed to ammonia and ethanol gases. The responses of the sensors to 1000 ppm of hydrogen gas at different operating temperatures (25 °C – 100 °C) were studied. Results show that a good sensitivity towards hydrogen gas was obtained with Fe doped SnO_2 thin film sensor at an optimal operating temperature of 75 °C. Response time of the sensor and its stability were also studied.

1. Introduction

Tin oxide (SnO_2) is a wide band-gap (~3.5 eV) compounds with metal-like conductivity and widely studied due to its potential applications as: conventional gas sensor due to its high reactivity with environmental gases [1]; catalyst for hydrocarbons oxidation [2], and an excellent optical transparency and high chemical stability have been recognized as very promising materials with widespread technological applications [3,4].

SnO_2 has been established as the predominant sensing material for the gases like CO, C_2H_5OH, NO etc. The basic sensing principle behind metal oxide based thin or thick film is that there will be a change in the electrical resistance due to gas reacting with negatively charged oxygen that is adsorbed on the surface of the metal oxide nanoparticles [5–10]. It is generally accepted that increasing the surface/bulk ratio by decreasing the grain size of rutile SnO_2 nanoparticles is crucial for achieving high-sensitivity in gas sensors. One of the other most common ways to modify the characteristics of the material is introducing dopants into the structure. Many results have shown that several additives (cations: Fe, Cu, Co, Cr, Al, Mn, Mg; anions: P, S) can lead to an increase of the surface area of SnO_2 sensors.

Doped SnO_2 thin films are extensively studied in the recent times due to its crystallinity, tetragonal rutile structure and gas sensing application. SnO_2 thin films are prepared by the various techniques such as reactive sputtering, spray pyrolysis, chemical vapour deposition, laser ablation and sol-gel having its own importance [11-14]. Sol gels have been used extensively as. Among these techniques, as it is economical, simple and energy saving method to deposit high quality films, simple experimental arrangement, easy control on film thickness with a high porosity area which can improve the efficiency of the sensors, greater homogeneity and more purity.

In this study, Fe-doped SnO_2 thin films with varying concentrations of iron were grown by sol–gel dip-coating technique on the glass substrates. H_2 gas-sensing properties of the as-grown Fe-doped SnO_2 thin films with varying concentrations of Fe were investigated.

2. Experimental Methods

2.1 Sol-Gel Synthesis of SnO_2 Nanocrystalline Thin Films

SnO_2 semiconductor thin film coating on the Pyrex glass (silica) slides (substrate) was conducted via sol–gel dip-coating technique. Tin-isopropoxide (10% w/v) in *iso*-propanol and toluene was purchased from Aldrich chemicals and used as-received. Pyrex glass slides, with roughness of ±10 nm, were received from Fisher Scientific. Small glass substrates (1 cm×1 cm), were cut from the glass slides for the dip-coating experiments. The glass substrates were ultrasonically cleaned, first in acetone and then in *iso*-propanol. The pre-cleaned substrates were dipped in the solution of tin-isopropoxide in *iso*-propanol and toluene, corresponding to the concentration 0.25 M of tin-isopropoxide, using a dip-coater with a withdrawal speed of 150 cm/min. The gel films were dried at 200 °C for 1 h in air. The substrates were dip-coated again using the same solution under similar conditions and then dried again at 200 °C for 1 h in air. The dried gel films were fired at 450 °C in air. The samples were heated at a rate of 30 °C/min upto 450 °C, held at that temperature for 2 h, and then cooled to room temperature inside the furnace. Finally, a thin layer of Pt was sputtered for 10 s on some of the semiconductor thin films using a sputter coater.

Table 1 Details of the deposition parameters of Fe-doped SnO_2 thin films

Parameters	Particulars
Concentration of tin-isopropoxide solution	0.25 M
Temperature at which films dried	200 °C
Time for films drying	1 h
Annealing temperature	450 °C
Film thickness	500 mm

2.2 Characterization

All the characterization techniques described below were employed after firing the sol–gel dip-coated Fe-doped SnO_2 thin films at 450 °C for 2 h. X-Ray power diffraction (XRD) analysis conducted on a Rigaku MiniFlex 600 X-Ray diffractometer with Cu-Kα radiation (λ = 1.5418 Å) as X-Ray source (at 20kV and 20 mA) in the scanning angle (2θ) range from 20° to 80°. The mean crystallite size calculated using Debye-Scherer formula,

$$D = \frac{0.95\lambda}{\beta Cos\theta} \quad (1)$$

*Corresponding Author:pawarmahendrasingh22@gmail.com(M.J. Pawar)

https://doi.org/10.30799/jnst.280.20060102

where, λ is the X-ray wavelength, θ is the Bragg diffraction angle and (in radians) is the full width at half maximum. The morphological analysis is done by field emission scanning electron microscopy (FESEM). The high-resolution transmission electron microscopy measurements are obtained on JEOL JEM-2100 microscope operated at 200 kV.

2.3 Gas Sensitivity Measurement

Gas response measurements of the samples are carried out as follows: The films are loaded in the sensing chamber with four probe leads attached. The film is heated in the chamber with atmospheric air as ambient and then in the ambience of H_2 gas. Resistance measurement and gas sensing response of the samples are carried out at different temperatures using Keithley 2400 source meter. The sensor response to a particular gas concentration is defined as,

$$S\% = \frac{R_a - R_g}{R_a} \times 100 \quad (2)$$

where, R_a and R_g are the resistances of the sample in the absence and presence of the test gas respectively.

3. Results and Discussion

Typical XRD patterns of the as-prepared SnO_2 samples are shown in Fig. 1 where one can see that they are identically similar except in peak intensities. The cassiterite phase of SnO_2 is identified, having no evidence of impurity regardless of dopant concentration. The diffraction peaks corresponding to Fe_2O_3 cannot be seen in XRD patterns, in the studied Fe concentration range less than 4 wt.%. It can be seen that the diffraction peaks become weaker and broader with the increasing amount of dopant, which indicate that Fe^{3+} doping suppress the growth of large SnO_2 crystallites.

Table 2 Crystallite size, lattice parameters of undoped and Fe doped SnO_2 Thin Films

Sample	Crystallite size (nm)	Cell volume (Å³)	a/c (Å)
SF	24.3	71.7522	1.4891
SF-1	23.7	71.7687	1.4878
SF-2	16.4	71.7734	1.4876
SF-3	12.6	71.4211	1.4870

Table 1 gives the information about lattice related parameters of pure and Fe-doped SnO_2 obtained from XRD data, where the crystallite size calculated from using the Scherrer formula. It is observed that the crystallite size decreases with increasing Fe-doping concentrations. This may be because of the fact that the dopant atoms exert a drag force on boundary motion and grain growth [15]. Hence addition of Fe element decreases the particle mobility on formation and thereby inhibits the growing-up of SnO_2 crystallites. When on the addition of dopant, crystallite size becomes less in the range of nano-scale, it is likely that the defects get introduced is found to be more in undoped films. Crystallite size is calculated from Scherrer formula, for undoped and doped SnO_2 films (Table 2) agree nearly with the values calculated from Williamson-Hall method.

To understand how the doping affects the morphology of the SnO_2 active layers, a morphological characterization based on scanning electron microscopy analysis was performed. Fig. 2 depicts the morphology of Fe-doped SnO_2 films at different concentrations, deposited at a substrate temperature 450 °C.

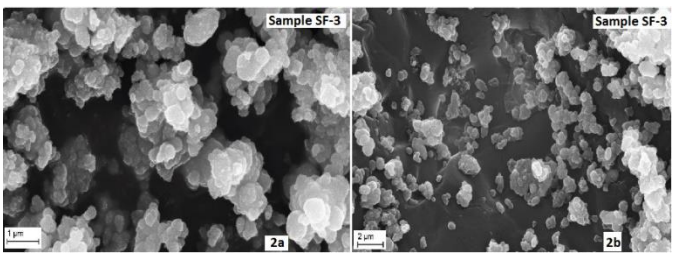

Fig. 2 SEM images of Fe doped SnO_2 thin films

The SEM images for lower Fe concentration (sample SF-3 at different magnifications) show that the distribution of smaller grains is not uniform but at higher levels (3 wt.% Fe), the smaller grains are more uniform and regular in size as shown in Fig. 2. It was observed that micrograph of sample SF-2 consist of mixed sized, less densely packed and polygon shaped grains. The films deposited at higher deposition temperatures have more uniform grains of larger size. The micrographs recorded for the different samples show that the films are essentially homogeneous, and made up of grains and voids. The voids within the film structure provide conduction paths for gas molecules to flow in from the environment. Conductivity of the films is due to the flow of current along the conducting paths of the constituents of the film that are formed randomly by connecting the grains together. As the concentration of Fe is increased to 3 wt.% (sample SF-3), the films become denser and closely packed (Fig. 2). In addition, the SEM picture indicates that the surface of the sample is porous. This clearly indicates that the metal dopant together with deposition temperature modifies the morphology and the sensing action.

The structural properties of doped and undoped SnO_2 films have a significant effect on the electrical and gas sensing property and for this reason structure and grain size measurements on the films were carried out. The relation between dopant weight percentage and crystallite size is plotted in Fig. 3. From the Fig. 3, it can be seen that as the crystallite size decreases with increase in the dopant weight percentage.

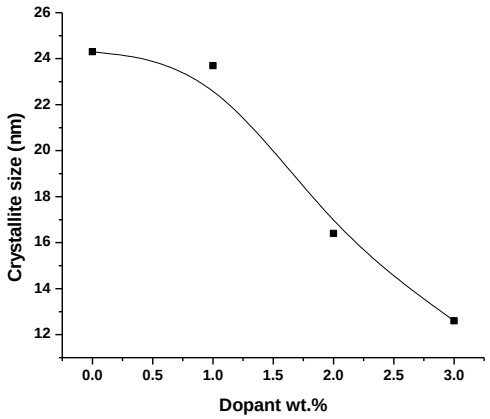

Fig. 3 Effect of dopant wt.% on crystallite size doped and undoped SnO_2 sensors

To investigate the gas sensing properties of Fe doped SnO_2 samples the fabricated films are loaded into the conductivity chamber. For measurements, the sample is kept inside the sensing chamber to attain the desired operating temperature under a pressure of 10^{-1} Torr. The surface resistance is allowed to equilibrate at the operating temperature for a reasonably long time prior to gas exposure. This value of resistance is defined as the initial equilibrium resistance in the absence of the test gas (Ra). Hydrogen gas was injected into the chamber roughly for 60 seconds to create a concentration of 1000 ppm and the resistance of the gas sensor (R_g) was continuously recorded for 10 minutes starting from the gas injection moment and is compared with the initial resistance. The exposure time to target gas was 10 minutes.

While gas sensitivity measurement, initially, the electrical resistances of the Fe doped SnO_2 films were high and on exposure to H_2 gas, an abrupt fall of the film resistance was observed. It is also observed that the electrical resistance gets saturated in less than 2 minutes. Fe-doped SnO_2 samples were found to be more sensitive to H_2 gas than undoped SnO_2 sample. Sensitivity heavily depends on the operating temperature of the sensors. The measurements are repeated at different operating temperatures as 25, 50, 75 and 100 °C to study the variation. The sensors reach the maximum sensitivity to H_2 gas at the operating temperature of 75 °C which is much lesser than our previous results [16].

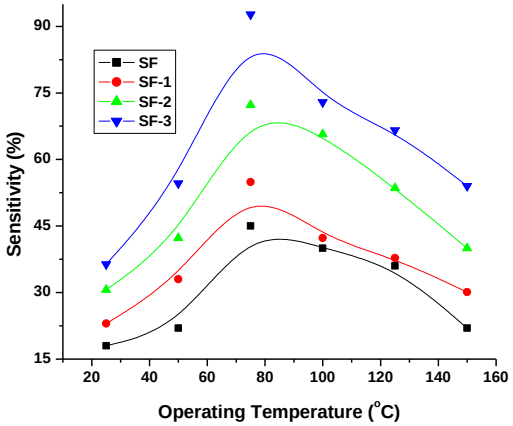

Fig. 4 Effect of operating temperature on sensitivity (%) of undoped and Fe-doped SnO_2 samples

https://doi.org/10.30799/jnst.280.20060102

Cite this Article as: S.V. Jagtap, A.S. Tale, S.D. Thakre, M.J. Pawar, Low Temperature hydrogen gas sensing performance of Fe-doped SnO_2 nanostructured thin films, J. Nanosci. Tech. 6(1) (2020) 866–868.

Fig. 4 shows the variation of sensitivity to 1000 ppm of H_2 gas with the operating temperature for undoped and Fe-doped SnO_2 samples. The sensitivity is found to increase with increase in operating temperature, attains a maximum at 75 °C followed by the decrease with further increase in the operating temperature. Also, with an increase in deposition temperature, the grain size increases causing a decrease in grain boundary potential and hence an increase in mobility. The decrease in grain boundary potential is also responsible for an increase in carrier concentration with deposition temperature, which results a decrease in resistance.

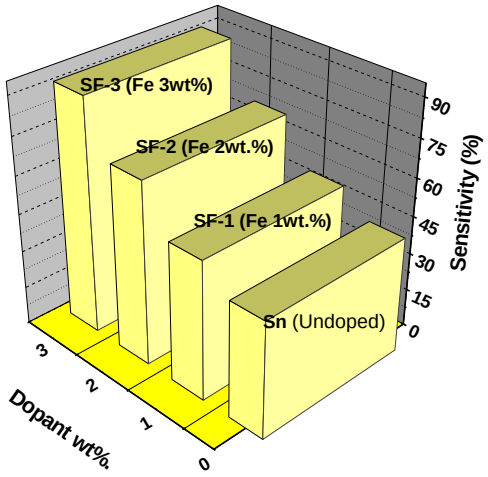

Fig. 5 Effect of dopant wt.% on sensitivity of SnO_2 samples at 75 °C

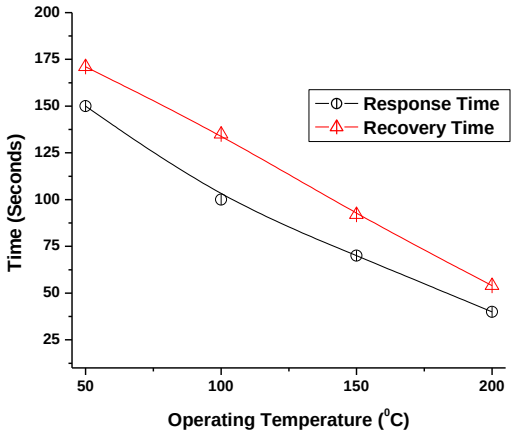

Fig. 6 The response and recovery times of the 3 wt.% Fe doped SnO_2 towards 1000 ppm hydrogen as a function of operating temperature

Fig. 5 shows the dependence of the sensitivity to the amount of Fe in SnO_2 for 1000 ppm of H_2 gas at 75 °C. The sensitivity of the Fe-doped SnO_2 increases when the amount of Fe is 3 wt.%. The enhanced sensitivity is due to the amount and distribution of the dopant. These results proved that a homogeneous distribution of the higher concentration of Fe in SnO_2 is advantageous to enhance sensitivity to H_2 gas.

Response and recovery times of the 3 wt.% Fe doped SnO_2 for 1000 ppm hydrogen are presented in Fig. 6. It presents a decaying behavior with considerable fast response and recovery times at high temperatures (200 °C). At low working temperature the response time is higher due to slow desorption of the formed water molecules on the surface especially at temperatures below 75 °C. Our results demonstrated faster response and recovery times in the order of 150–170 s for low temperature sensing which so considerable compare to 40 min recovery time is. It can be attributed to the facilitate occupancy and desorption of H_2 molecules at grain boundaries on the large surface area of prepared samples. However, the obtained results of the response magnitudes and the working temperature are not as good as our previous work on thin film sensors.

4. Conclusion

In this study, Fe-doped SnO_2 nanostructured thin films with different dopant amounts were synthesized by sol–gel dip-coating technique. By using X-ray diffraction and electron microscopy studies, it is found that Fe^{3+} doping can suppress the growth of large SnO_2 crystallites and assist in a uniform growth of agglomerated grains. The gas sensing properties to H_2 is tested and found that 3 wt. % Fe-doped SnO_2 exhibit the best gas sensing properties which can be attributable to enhanced capability of adsorbing oxygen by Fe on the surface. This implies a good potential of the Fe-dopant in SnO_2 films, for practical H_2 gas sensing applications at 75 °C.

References

[1] B. Bahrami, A. Khodadadi, M. Kazemeini, Y. Mortazavi, Enhanced CO sensitivity and selectivity of gold nanoparticles-doped SnO_2 sensor in presence of propane and methane, Sens. Actuators B 133 (2008) 352-356.
[2] R. Pearce, W.R. Patterson, Catalysis and chemical processes, Leonard Hill, Glasgow, 1981.
[3] H.L. Hartnagel, Semiconducting transparent thin films, Institute of Physics Publishing, Philadelphia, 1995.
[4] S.B. Ogale, R.J. Choudhary, J.P. Buban, S.E. Lofland, S.R. Shinde, et al., High temperature ferromagnetism with a giant magnetic moment in transparent co-doped $SnO_{2-\delta}$, Phys. Rev. Lett. 91 (2003) 077205:1-4.
[5] N. Hongsith, E. Wongrat, T. Kerdcharoen, S. Choopun, Sensor response formula for sensor based on ZnO nanostructures, Sens. Actuator B: Chem. 144(1) (2010) 67–72.
[6] S.B. Kondawar, S.P. Agrawal, S.H. Nimkar, H.J. Sharma, P.T. Patil, Conductive polyaniline-tin oxide nanocomposites for ammonia sensor, Adv. Mater. Lett. 3(5) (2012) 393–398.
[7] J.R. Brown, M.T. Cheney, P.W. Haycock, D.J. Houlton, A.C. Jones, E.W. Williams, The gas-sensing properties of tin oxide thin films deposited by metallorganic chemical vapor deposition, J. Electrochem. Soc. 144(1) (1997) 295–299.
[8] A.J. Galdikas, V. Jasutis, S. Kaciulis, Peculiarities of surface doping with Cu in SnO_2 thin film gas sensors, Sens. Actuator B: Chem. 43(1–3) (1997) 140–146.
[9] M.I. Ivanovskaya, P.A. Bogdanov, D.R. Orlik, A.C. Gurlo, V.V. Romanovskaya, Structure and properties of sol-gel obtained SnO_2 and SnO_2-Pd films, Thin Solid Films 296(1-2) (1997) 41–43.
[10] S.D. Bakrania, M.S. Wooldridge, The effects of the location of Au additives on combustion-generated SnO_2 nanopowders for CO gas sensing, Sensors 10(7) (2010) 7002–7017.
[11] A. Dieguez, A.R. Rodriguez, J.R. Morante, J. Kappler, N. Barsan, W. Copel, Nanoparticle engineering for gas sensor optimisation: improved sol–gel fabricated nanocrystalline SnO_2 thick film gas sensor for NO_2 detection by calcination, catalytic metal introduction and grinding treatments, Sens. Actuator B: Chem. 60 (1999) 125-137.
[12] D.G. Rickerby, M.C. Horrillo, Crystallite size distributions and lattice defects in r.f. sputtered nanograin TiO_2 and SnO_2 films, J. Nanostruct. Mater. 10 (1998) 357-363.
[13] W.S. Hu, Z.G. Liu, J.G. Zheng, X.B. Hu, X.L. Guo, W. Gopel, Preparation of nanocrystalline SnO_2 thin films used in chemisorption sensors by pulsed laser reactive ablation, J. Mater. Sci.: Mater. Electron. 8 (1997) 155-157.
[14] G. Sberveglieri, G. Faglia, S. Groppelli, P. Nelli, C. Perego, Oxygen gas sensing properties of undoped and Li-doped SnO_2 thin films, Sens. Actuators B: Chem. 13-14 (1993) 117-120.
[15] Y.M. Chiang, D.P. Birnie III, W.D. Kingery, Physical ceramics: Principles for ceramic science and engineering, Physics Ceramics, John Wiley, New York, 1997.
[16] S.V. Jagtap, A.S. Tale, S.D. Thakare, M.J. Pawar, Effect of annealing temperature on hydrogen gas sensitivity of nanocrystalline SnO_2 thin films, J. Nanosci. Tech. 5(4) (2019) 802-805.

https://doi.org/10.30799/jnst.280.20060102

Cite this Article as: S.V. Jagtap, A.S. Tale, S.D. Thakre, M.J. Pawar, Low Temperature hydrogen gas sensing performance of Fe-doped SnO_2 nanostructured thin films, J. Nanosci. Tech. 6(1) (2020) 866–868.